Cerebral Cortex, 2022, 32, 1508–1519

https://doi.org/10.1093/cercor/bhab303
Advance Access Publication Date: 7 September 2021
Original Article

ORIGINAL ARTICLE

Partially Preserved Processing of Musical Rhythms in REM but Not in NREM Sleep

Rebeca Sifuentes-Ortega[1], Tomas Lenc[2], Sylvie Nozaradan[2] and Philippe Peigneux[1]

[1]UR2NF – Neuropsychology and Functional Neuroimaging Research Unit at CRCN – Center for Research in Cognition & Neurosciences, and UNI – ULB Neuroscience Institute, Université Libre de Bruxelles (ULB), 1050 Brussels, Belgium and [2]Institute of Neuroscience (IONS), Université Catholique de Louvain, 1200 Brussels, Belgium

Address correspondence to Rebeca Sifuentes-Ortega, UR2NF - Neuropsychology and Functional Neuroimaging Research Unit, CRCN Université Libre de Bruxelles (ULB), Av. F. Roosevelt 50, CP 191, 1050 Bruxelles, Belgium. Email: rebeca.sifuentes.ortega@ulb.be

Abstract

The extent of high-level perceptual processing during sleep remains controversial. In wakefulness, perception of periodicities supports the emergence of high-order representations such as the pulse-like meter perceived while listening to music. Electroencephalography (EEG) frequency-tagged responses elicited at envelope frequencies of musical rhythms have been shown to provide a neural representation of rhythm processing. Specifically, responses at frequencies corresponding to the perceived meter are enhanced over responses at meter-unrelated frequencies. This selective enhancement must rely on higher-level perceptual processes, as it occurs even in irregular (i.e., syncopated) rhythms where meter frequencies are not prominent input features, thus ruling out acoustic confounds. We recorded EEG while presenting a regular (unsyncopated) and an irregular (syncopated) rhythm across sleep stages and wakefulness. Our results show that frequency-tagged responses at meter-related frequencies of the rhythms were selectively enhanced during wakefulness but attenuated across sleep states. Most importantly, this selective attenuation occurred even in response to the irregular rhythm, where meter-related frequencies were not prominent in the stimulus, thus suggesting that neural processes selectively enhancing meter-related frequencies during wakefulness are weakened during rapid eye movement (REM) and further suppressed in non-rapid eye movement (NREM) sleep. These results indicate preserved processing of low-level acoustic properties but limited higher-order processing of auditory rhythms during sleep.

Key words: EEG, frequency tagging, musical meter, rhythm processing, sleep

Introduction

It is well established that the processing of basic auditory information is preserved during sleep, in which neurons from primary auditory cortices keep responding to incoming stimuli like during wakefulness (Peña et al. 1999; Issa and Wang 2008; Nir et al. 2015). Accordingly, event-related potential (ERP) components reflecting early sensory processing resemble those evoked during wakefulness, whereas late latency components reflecting higher-order cognitive processes undergo greater distortions during the different sleep stages (Atienza et al. 2001). Still, at a higher processing level, incoming information continues being at least partially discriminated by the sleeping brain based on relevance or salience. For example, differential brain responses to the subject's own name (Perrin et al. 1999) or semantically incongruent words and phrases have been reported during stage 2 of non-rapid eye movement (NREM) sleep and in rapid eye movement (REM) sleep (Bastuji et al. 2002; Daltrozzo et al. 2012). Additionally, a continued appraisal of paralinguistic features such as familiar versus unfamiliar voices has been observed during all sleep stages (Blume et al. 2018).

Furthermore, electrophysiological motor preparation-related responses to task-relevant semantic information (Kouider et al. 2014) and selective amplification of informative over meaningless competing speech streams were found during light NREM sleep and REM sleep (Legendre et al. 2019; Koroma et al. 2020), suggesting that high-order information processes still take place during sleep.

Nonetheless, the extent to which high-order information can be processed during sleep remains disputed. For instance, the parsing of high-order linguistic structures such as words, phrases, and sentences is disrupted during all stages of sleep, whereas the tracking of low-level acoustic properties of speech (i.e., syllabic rate) is relatively preserved regardless of its intelligibility (Makov et al. 2017). Accordingly, beyond the primary auditory cortex, high-order language processing regions exhibit reduced activation when presented with verbal stimuli during sleep (Portas et al. 2000; Wilf et al. 2016). Besides language processing, the capacity to abstract temporal structure and regularities within relatively long auditory streams seems also impaired during sleep. For instance, the ability to detect violations of global regularities in auditory signals within a local/global paradigm is abolished during sleep, whereas adaptation to local changes is partially preserved (Strauss et al. 2015). Similarly, the extraction of statistical regularities from auditory streams is absent during NREM sleep, whereas responses to individual tones within the streams are preserved (Farthouat et al. 2018).

Considering temporal structures in particular, listening to musical rhythms often induces high-level representations such as the meter. Such pulse-like meter perceived when listening to music is often manifested at the behavioral level by a spontaneous periodic entrainment of the motor system (e.g., periodically tapping, or bobbing the head to the meter) (Nozaradan 2014). At the neural level, entrainment to musical rhythms can be reflected by activity preferentially synchronized to meter frequencies perceived in the rhythms (Nozaradan et al. 2011, 2012; Tierney and Kraus 2014; Meltzer et al. 2015). By using the frequency-tagging approach, studies consistently showed that electroencephalography (EEG) responses to rhythms designed to induce a spontaneous perception of meter are elicited at multiple frequencies, corresponding to the exact same frequencies contained in the acoustic envelope of the rhythms (Nozaradan et al. 2012, 2017, 2018; Lenc et al. 2018). More importantly, there is increasing evidence that the amplitude of neural responses elicited at meter-related frequencies is selectively enhanced in the EEG spectrum relative to the remaining envelope frequencies that are irrelevant for meter perception (Nozaradan et al. 2012, 2017, 2018; Lenc et al. 2018). Furthermore, in the case of more irregular, syncopated, rhythms where the perceived meter frequencies are not strongly supported by acoustic cues, cortical responses at meter frequencies are still enhanced regardless of their prominence within the modulation spectrum of the rhythm, thus controlling for low-level acoustic confounds (Nozaradan et al. 2017, 2018; Lenc et al. 2018). These results are compatible with the view that the neural representation of the temporal structure of complex irregular sequences is supported by the endogenous synchronization of cortical areas to the meter frequencies, rather than being merely stimulus driven (Large et al. 2015; Tal et al. 2017). Hence, capturing selective enhancement of brain responses to meter-related frequencies provides a direct measure of high-level perceptual auditory processing in the absence of explicit behavioral responses that cannot be provided during sleep. Specifically, these higher-level processes can be isolated by comparing the selective neural enhancement of meter frequencies between regular (i.e., unsyncopated) rhythms where the meter consistently coincides with acoustic cues and more irregular (i.e., syncopated) rhythms where the perceived meter is not strongly supported by acoustic cues. Building on these prior findings, we investigated the emergence of high-order neural representations of meter across different sleep stages. To this end, we recorded EEG frequency-tagged responses elicited by syncopated and unsyncopated rhythms during NREM and REM sleep stages and wakefulness.

Materials and Method

Participants

Eighteen healthy participants (6 male, mean age 24.7 ± 4.2, range 20–35 years) with reported normal hearing, free of medication, and no history of neurological or psychiatric disorders took part in the study. Four participants were excluded from the analysis due to poor sleep during the experimental night ($n = 2$) or technical issues during the experiment ($n = 2$). The final sample consisted of 14 participants (5 male, mean age 24.2 ± 3.6, range 20–33 years) with good sleep quality (Pittsburgh Sleep Quality Index; Buysse et al. 1989, global mean score 3.1 ± 1) and neutral to moderate chronotype (Morningness–Eveningness Questionnaire; Horne and Östberg 1976, mean score 51.7 ± 8.9, range 36–66). All participants gave their written informed consent before starting this study, approved by the ULB-Erasme Hospital Ethics Committee (Ref.: P2018/085). They received monetary compensation after completion of the experiment.

Auditory Stimuli

The auditory stimuli created in Matlab R2017b (https://www.mathworks.com) consisted of 2 non-isochronous rhythms of 2.4-s duration looped continuously into 40.8-s sequences. These rhythms were constituted by a repeated chord with 3 partials (f1 = 209 Hz; f2 = 398 Hz; f3 = 566 Hz). The chord was modulated in amplitude, generating 12 events lasting 200 ms each, which were either audible (linear ramp onset and offset lasting 10% of the event duration, and modulation depth of 90%, from 0.1 to 1) or silent (amplitude kept at 0.1) (Fig. 1A). Previous work using tapping tasks showed that these 2 rhythms induce the perception of a consistent meter across participants. The perceived meter consists in periods corresponding to the shortest inter-onset intervals making up the sequences (200 ms = 5 Hz frequency) and grouping of these intervals by 2 (2 × 200 ms = 400 ms period = 2.5 Hz frequency), 4 (4 × 200 ms = 800 ms = 1.25 Hz), and 12 intervals (2.4 s = 0.416 Hz) (Nozaradan et al. 2012, 2018; Lenc et al. 2018), and these frequencies are thus categorized as relevant for meter perception ("meter-related frequencies") in further analysis of the stimulus and the EEG. Moreover, the specific arrangement of acoustic and silent events in the sequences gives rise to 2 distinct rhythms. Namely, a regular, unsyncopated rhythm in which the perceived meter periods match the physical arrangement of acoustic event onsets, and an irregular, syncopated rhythm in which the perceived meter periods are not strongly cued by its physical structure (Lenc et al. 2018, 2020). Consequently, the latter rhythm is considered as more complex, since meter perception must rely on endogenous higher-level processes, beyond low-level processing of the acoustic input.

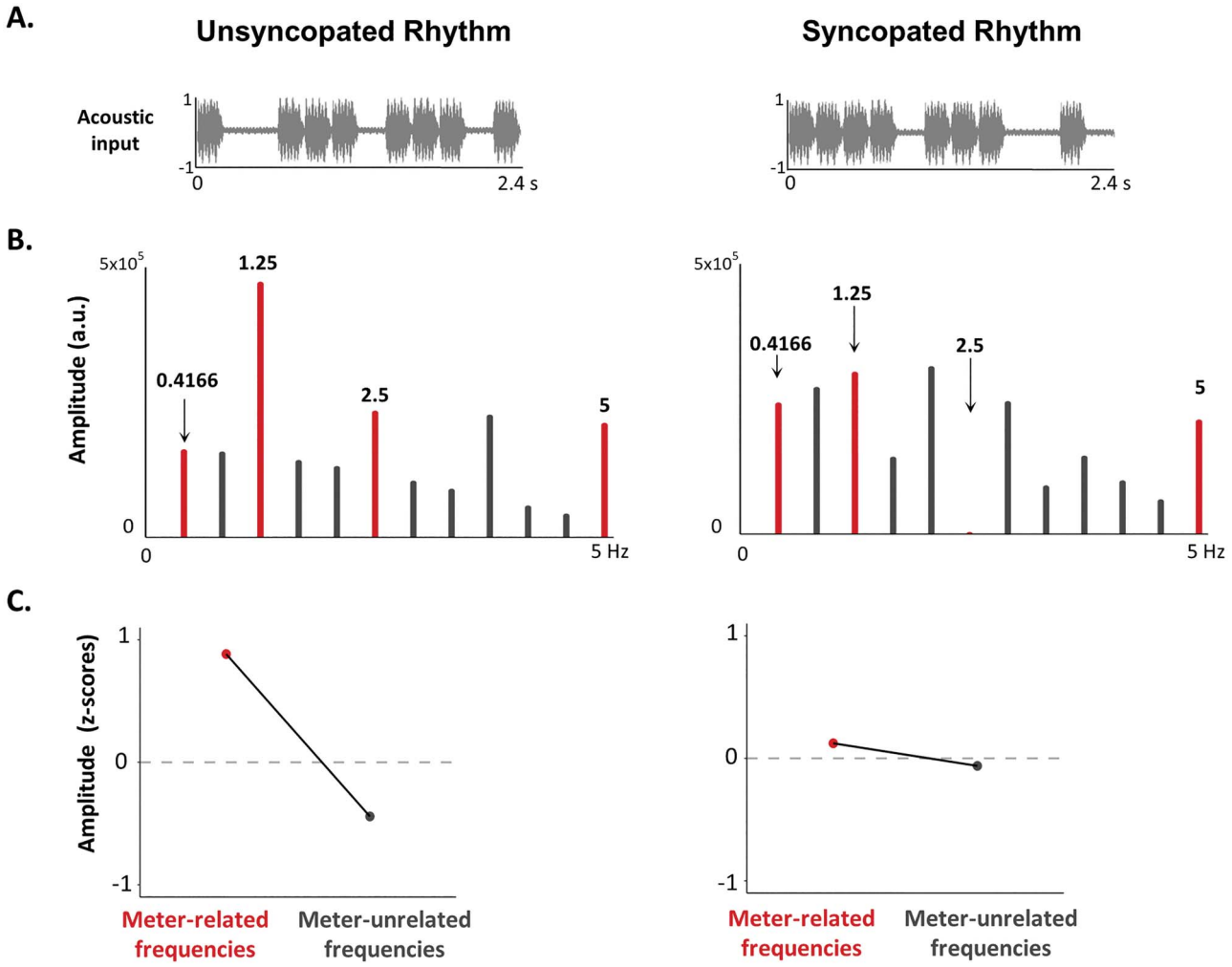

Figure 1. Stimuli design. Two 2.4-s rhythmic patterns looped into trials of 40.8 s were presented during nocturnal sleep and wakefulness. (*A*) The patterns consisted of an amplitude-modulated chord giving rise to "acoustic" and "silent" events lasting 200 ms. These events were arranged in a way to make up an unsyncopated (left) and a syncopated rhythm (right). (*B*) Frequency spectra of the sound envelopes up to the frequency corresponding to the shortest inter-onset interval. Meter-related and meter-unrelated frequencies are depicted in red and gray, respectively. As opposed to the unsyncopated rhythm, the syncopated rhythm does not show predominant acoustic energy at the meter frequencies as compared to the other envelope frequencies. (*C*) Mean z-score amplitudes of meter-related and meter-unrelated frequencies of the 2 rhythmic patterns. Note that the difference in relative prominence of meter-related over meter-unrelated frequencies is greater in the unsyncopated rhythm as compared to the syncopated one.

Experimental Design

Prior to the experiment, participants were asked to keep regular sleeping habits. This was verified by means of actimetry (wGT3X-BT, ActiGraph, USA) and a sleep log that participants completed for 3 days before the beginning of the experiment. The experimental session began at 21:30 h with the placement of EEG electrodes, electrooculography (EOG), and electromyography (EMG). After receiving instructions, participants went to sleep in a soundproof, magnetic-shielded chamber (Frankonia, Germany). Polysomnography (PSG) was continuously monitored, and blocks of auditory stimulation were delivered after at least 2 min of clearly identifiable stages N2 and N3 of NREM sleep, and REM sleep. The 2 rhythms, one regular or unsyncopated, and the other irregular or syncopated, were played in blocks of 9 trials each lasting 40.8 s and with 3 s of silence in between. Block presentation order was counterbalanced within each sleep/wake condition across participants. Whenever signs of arousal or sleep stage transition were observed in the PSG, the stimulation block was interrupted and presented at the next opportunity in order to achieve at least 1 complete block of stimulation for each rhythm and condition. Participants slept 8 h on average. Thirty minutes after awakening, they were comfortably seated on a chair, were asked not to move, and keep the same position during the final blocks of stimulation that consisted in the presentation of each rhythm. Participants were also asked to fixate their gaze to a point on the wall in front of them while listening attentively to the rhythms.

Sound Analysis to Determine Frequencies of Interest

The frequencies of interest for the EEG analysis were determined by extracting the acoustic envelope of the 40.8-s sequences by means of the Hilbert transform, as implemented in Matlab, and then by transforming it into the frequency domain by using

a discrete Fourier transform. For each rhythm, the resulting spectrum contained 12 envelope frequencies ranging from the slowest frequency of 0.416 Hz corresponding to the repetition frequency of the entire rhythmic pattern (2.4-s period), and its harmonics up to the fastest 5 Hz frequency corresponding to the event rate of the rhythms (200 ms period; Fig. 1B). These envelope frequencies were then categorized as meter-related and meter-unrelated, based on the meter periods consistently identified as constituting the perceived meter induced by these rhythms. Meter-related frequencies as defined above thus corresponded to the 1st, 3rd, 6th, and 12th frequencies of the envelope spectrum, whereas the 8 remaining frequencies were categorized as meter-unrelated, since they did not correspond to the perceived meter periods (Nozaradan et al. 2012, 2018; Lenc et al. 2018).

Importantly, although the 2 rhythmic patterns are assumed to induce perception of musical meter at consistent periods across individuals, they may provide the listener with different amounts of direct sensory cues to this perceived metric structure (Nozaradan et al. 2012, 2016, 2018; Lenc et al. 2018, 2020). Therefore, quantifying the relative prominence of the meter-related frequencies over the other, meter-unrelated frequencies in the 2 acoustic sequences is critical to further interpret the relative prominence of the meter-related frequencies observed in the neural activity, that is, to interpret the degree of transformation from the acoustic envelope to the captured EEG. Indeed, observing prominent neural activity at meter-related frequencies in response to a rhythmic sequence where the meter-related frequencies are already prominent in the acoustic envelope can be trivially explained by low-level properties of the auditory system faithfully tracking these prominent acoustic features. In contrast, observing a selective enhancement of the meter-related frequencies in the neural response to a rhythmic sequence where the meter-related frequencies are not prominent in the input in the first place would allow us to control for such an acoustic confound and capture higher-level perceptual processes that cannot be easily explained by low-level auditory processing (Lenc et al. 2020, 2021). To measure the relative prominence of meter frequencies, amplitudes at the 12 frequencies corresponding to the stimulus modulation spectrum were converted to z-scores as follows: ([x] – [mean across the 12 frequencies])/[SD across the 12 frequencies]. A higher z-score at a specific frequency indicates that the response at that frequency stands out prominently relative to the whole set of frequencies in the modulation spectrum. The z-scores for meter-related frequencies were averaged to obtain an index of their relative prominence in the modulation spectra. In the unsyncopated rhythm, this meter z-score was 0.883, whereas the meter z-score of the syncopated rhythm was 0.123, thus confirming that the syncopated rhythm did not contain prominent acoustic cues to the meter periods (Fig. 1C).

In addition to the envelope frequencies contained in the structure of the rhythms, we also aimed at investigating fast frequency-following responses derived from the partial frequencies of the amplitude-modulated chord of the rhythms (i.e., f1, f2, f3), which are thought to reflect earlier stages of auditory processing (Coffey et al. 2019). Simultaneously capturing these fast responses was allowed by the high sampling rate of our EEG setup (i.e., 8192 Hz, see EEG Recording section). Such responses are assumed to mainly originate from subcortical relays of the auditory pathway such as the inferior colliculus (Skoe and Kraus 2010), in contrast with the responses to acoustic envelopes that are assumed to originate from cortical sources (Nozaradan et al. 2017). These frequency-following responses can be recorded alongside the "cortical" responses to the acoustic envelope, and the 2 types of responses can be disentangled based on their respective frequencies (frequencies of the tones conveying the rhythm vs. frequencies of the envelope making up the rhythm). This method has recently been proposed as a way to understand how auditory representations of rhythms are transformed across different levels of auditory processing (Nozaradan et al. 2016, 2018). To determine the frequency-following responses expected in the EEG, a discrete Fourier transform was applied to the rhythmic sequences. The frequency spectrum showed 3 peaks of acoustic energy at 209, 398, and 566 Hz, flanked by sideband frequencies that reflected the amplitude modulation of each partial by the rhythmic envelope (Nozaradan et al. 2018). We also examined distortion products (i.e., f3 – f2, f3 – f1, f2 – f1) generated at the inner ear (or otoacoustic emissions; Nozaradan et al., 2018). Distortion products correspond to frequencies that are not present in the stimulus spectrum but are elicited by cochlear nonlinearities, which thus ensure that these high-frequency responses are free of any possible electrical artifact generated by the sound stimulation device. Importantly for the purpose of the current study, these distortion products are also flanked by sideband frequencies reflecting the rhythmic amplitude modulation of the distortion products (Nozaradan et al. 2018).

Auditory Stimulation

The rhythmic sequences were presented binaurally through electromagnetically shielded insert earphones (ER-2, Etymotic Research, USA) using the Psychophysics Toolbox extension version 3 (Brainard 1997) running in Matlab. Sound intensity was adjusted before sleep to a level that participants found comfortable and that they expected would not disturb their sleep (~45 dB sound pressure level). To avoid awakening participants due to the onset of the auditory sequences, constant white noise was delivered throughout the night at a comfortable level (~33 dB SPL). Importantly, sound and background white noise intensity remained constant across sleep and wake conditions for each participant.

EEG Recording

Continuous EEG recordings were performed using an Active-Two Biosemi System (Biosemi, The Netherlands) with active Ag-AgCl electrodes on scalp locations C3, C4, Cz, FCz, and Fz according to the extended version of the 10-20 international system (Chatrian et al. 1985). Signals were referenced to the Common Mode Sense electrode and digitized at 8192 Hz sampling rate. Since active electrodes prevent the generation of impedance-dependent nuisance voltages, we did not control for electrode impedances but rather kept the direct-current offset below 20 mV during electrode placement. Exported signals from EEG channels were re-referenced offline to averaged mastoid channels. Only the signals from the 3 midline channels (Cz, FCz, Fz) were included in the frequency-following response analysis, as these locations have been previously shown to capture brainstem and cortical responses to auditory stimulation (Skoe and Kraus 2010; Nozaradan et al. 2018).

Sleep Scoring

To verify that auditory stimulation was correctly delivered at stages N2 and N3 of NREM sleep, and REM sleep, offline sleep scoring was performed on 30-s epochs according to standard

criteria (Berry et al. 2017) by an experienced researcher blind to trial onsets. EEG and EOG channels were high-pass filtered at 0.3 Hz and low-pass filtered at 45 Hz, and EMG was high- and low-pass filtered at 10 and 50 Hz, respectively. Offline scoring was used as the reference for subsequent EEG analyses, allowing us to exclude epochs of stimulation that did not correspond to the online assessment of sleep stimulation conditions (e.g., arousals or sleep stage transitions).

Frequency-Domain Analysis of EEG Responses

EEG processing was conducted following the approach described in Nozaradan et al. (2018) and carried out using Letswave6 (www.letswave.org) and Matlab. Continuous EEG recordings were high-pass filtered at 0.1 Hz with a second-order Butterworth filter to remove slow drifts in the signal. Stimulation trials were segmented into epochs ranging from 0 to 40.8 s time-locked to auditory stimulation onset. A notch fast Fourier transform (FFT) filter at 50 Hz and harmonics was applied to reduce line noise, and DC offset was removed from each epoch. Segmented artifact-free epochs were averaged in the time domain across trials for each participant and condition. This averaging procedure was used to enhance signal-to-noise ratio of the activity elicited by the stimulation while attenuating the contribution of activity not aligned to the stimulus across trials (Nozaradan et al. 2018). The obtained averaged waveforms were transformed in the frequency domain using FFT, yielding spectra of signal amplitudes (in μV) with approximately 0.02 Hz resolution (=1/40.8 s).

In order to obtain valid estimates of frequency-tagged responses elicited by periodic stimulation, the contribution of stimulation-unrelated residual background noise was reduced by subtracting the average amplitude at neighboring frequency bins relative to each frequency bin of the spectrum (bins 2–5 on both sides), separately for each participant, condition, and electrode. This noise subtraction procedure relies on the assumption that in the absence of periodic EEG responses to stimulation, the amplitude response at a given frequency bin should be similar to the mean amplitude of the surrounding bins (Mouraux et al. 2011; Nozaradan et al. 2012, 2018; Tierney and Kraus 2014). Noise-subtracted spectra were then averaged across all the scalp EEG channels (Fz, FCz, Cz, C3, and C4) for envelope-following responses analysis and across the 3 midline channels (Fz, FCz, and Cz) for the frequency-following responses analysis. Noise-subtracted averaged amplitudes at frequencies of interest (defined by the sound analysis) were then estimated for each condition and participant at the exact corresponding frequency bin of the EEG spectrum. As each epoch contained an integer number of repetitions of the 2.4-s rhythmic sequence (i.e., 17 repetitions in a 40.8-s trial), the frequency bins were exactly centered at the 12 frequencies constituting the envelope modulation spectrum of the unsyncopated and syncopated rhythms. Thus, envelope-following responses were estimated at the bins centered at the 12 frequencies of interest. The frequency-following responses were estimated at the closest bins to the frequencies of the 3 partials of the chord, their distortion products, and sideband frequencies.

Statistical Evaluation

First, we examined whether each rhythmic sequence elicited significant envelope-following and frequency-following responses in all conditions (stages N2 and N3 of NREM, REM sleep, and wakefulness). To this end, one-sample *t*-tests were performed to determine whether the amplitude of the responses was significantly different from zero across participants. These tests were performed given the assumption that in the absence of a significant response to the periodic sound stimulation, the noise subtraction method would lead to amplitudes distributed around zero (Mouraux et al. 2011; Nozaradan et al. 2012, 2018). Tests were performed by taking the amplitude averaged across meter-related frequencies (0.416, 1.25, 2.5, and 5 Hz) and meter-unrelated frequencies (8 remaining frequencies from the 12 frequencies of interest) expected in response to the presentation of the unsyncopated and the syncopated rhythms. Likewise, frequency-following responses were tested across the 3 partials of the chord, distortion products, and their respective sidebands, for each rhythm during the wake condition. To further characterize non-significant results, and determine whether these supported the null hypothesis over the alternative, Bayesian one-sample *t*-tests were performed in JASP (version 0.14.1; JASP Team 2020) with default priors. By convention, a Bayes Factor (BF_{01}) > 3 is considered to provide substantial evidence in favor of the null hypothesis, while a $BF_{01} < 0.333$ provides substantial evidence for the alternative hypothesis (Dienes 2014).

In order to compare the effect of state (wake, N2, N3, REM), meter (meter-related, meter-unrelated frequencies), and rhythm complexity (unsyncopated, syncopated) on EEG frequency-tagged responses, we performed linear mixed models with the *lme4* package (version 1.1-26; Bates et al. 2015) in R (version 3.6.1; R Core Team 2019). The model included state, meter, and rhythm as fixed effects as well as their interactions, and random intercepts for each participant. As the number of trials could differ between sleep and wake conditions, we weighted the amplitude values in each condition by the number of trials averaged per condition when estimating the model parameters by using the *weights* option of the *lmer* function (Tranchant et al. 2016). Significance of main effects and interactions was determined by running Type II Wald *F*-tests using the *Anova* function of the *car* package (version 3.0-10; Fox and Weisberg 2019). *P*-values were obtained using the Kenward–Roger approximation for degrees of freedom. Post hoc comparisons were performed using the *emmeans* package (version 1.6.1; Lenth 2021). Significance level was set at $P < 0.05$ and false discovery rate (FDR) correction was applied for multiple comparisons (Benjamini and Hochberg 1995).

Results

Sleep Parameters and Auditory Stimulation

Sleep parameters during the night of auditory stimulation and average number of 40.8-s artifact-free trials entered into the analysis per condition are reported in Tables 1 and 2. Participants were debriefed in the morning. Some of them recalled briefly hearing sounds during the night (as opposed to the continuous white noise, which was mostly heard in the beginning of the night while falling asleep). Auditory stimulation in N3 could not be achieved in 1 participant due to constant awakenings in the first half of the night. Therefore, analyses of responses during sleep stage N3 were performed on 13 participants.

Frequency-Tagged Responses to Rhythms Are Present in Wakefulness and in REM but not NREM Sleep

We first evaluated the magnitude of EEG responses elicited at the frequencies determined by the structure of the rhythmic sequences (i.e., the envelope modulation spectrum frequencies).

Table 1 Overnight sleep parameters

TST (min)	477.68 ± 12.87
Sleep latency (min)	10.5 ± 2.32
Stage 1 (%)	5.56 ± 0.61
Stage 2 (%)	46.84 ± 1.80
Stage 3 (%)	24.57 ± 1.44
REM (%)	23.02 ± 1.40
WASO (%)	10.28 ± 1.25

Data are expressed as means ± SEM; $N = 14$. TST, total sleep time; WASO, wake after sleep onset.

Table 2 Auditory stimulation trials

	Unsyncopated rhythm	Syncopated rhythm
Wake	7.9 ± 1.04	7.62 ± 1.04
Stage 2	8.4 ± 1.81	9.2 ± 1.35
Stage 3	9.39 ± 2.26	9.5 ± 1.51
REM	8.4 ± 0.88	8.9 ± 3.36

Average (±SD) number of 40.8-s trials entered into the analysis per condition ($N = 14$ in wake, N2, and REM states; $N = 13$ in N3).

Responses at the 12 envelope frequencies of interest were averaged for each participant and condition across meter-related frequencies (0.416, 1.25, 2.5, and 5 Hz) and meter-unrelated frequencies (8 remaining envelope frequencies). In line with previous work (Nozaradan et al. 2012, 2018; Lenc et al. 2018), the unsyncopated and syncopated rhythms elicited significant envelope-following responses at meter-related and meter-unrelated frequencies in the wake condition ($Ps < 0.01$, one-sample t-tests against zero), as shown in Table 3 and Figure 2A. In REM sleep, responses at meter-related frequencies in both unsyncopated ($P = 0.08$, $BF_{01} = 0.36$) and syncopated rhythms ($P = 0.08$, $BF_{01} = 0.33$) were no longer significant after FDR correction, although Bayes factors indicated support for the alternative hypothesis (i.e., for presence of frequency-tagged responses at meter frequencies). In contrast, responses at meter-unrelated frequencies in REM were nonsignificant ($P = 0.48$, $BF_{01} = 1.8$, and $P = 0.6$, $BF_{01} = 3.33$, for both rhythms, respectively). Finally, in NREM sleep, none of those responses were significantly elicited in N2 and N3 ($Ps > 0.53$, $BFs_{01} > 2.35$; Table 3). In summary, these results indicate that responses to both meter-related and meter-unrelated frequencies of the envelope of the rhythmic sequences were significantly elicited in wakefulness, whereas only responses to meter-related frequencies but not meter-unrelated frequencies persisted in REM sleep (with the limitation that these responses were no longer statistically significant after correction for multiple comparisons). In contrast, responses to the envelope of the rhythms, at both meter-related and unrelated frequencies, seem not to be elicited during stages 2 and 3 of NREM sleep (Fig. 2A).

Given the prominence of slow-wave activity (<1 Hz) during NREM sleep, and that the range of envelope frequencies investigated here partially overlapped with those frequencies, we performed an additional analysis on the same EEG epochs focusing on the 3 faster meter-related frequencies (i.e., responses at 0.416 Hz were excluded). A similar pattern of results emerged, with significant envelope-following responses at meter-related frequencies for both rhythms during wake ($Ps < 0.01$) and at meter-related frequencies for both rhythms during REM ($Ps < 0.03$). The results remained significant after FDR correction.

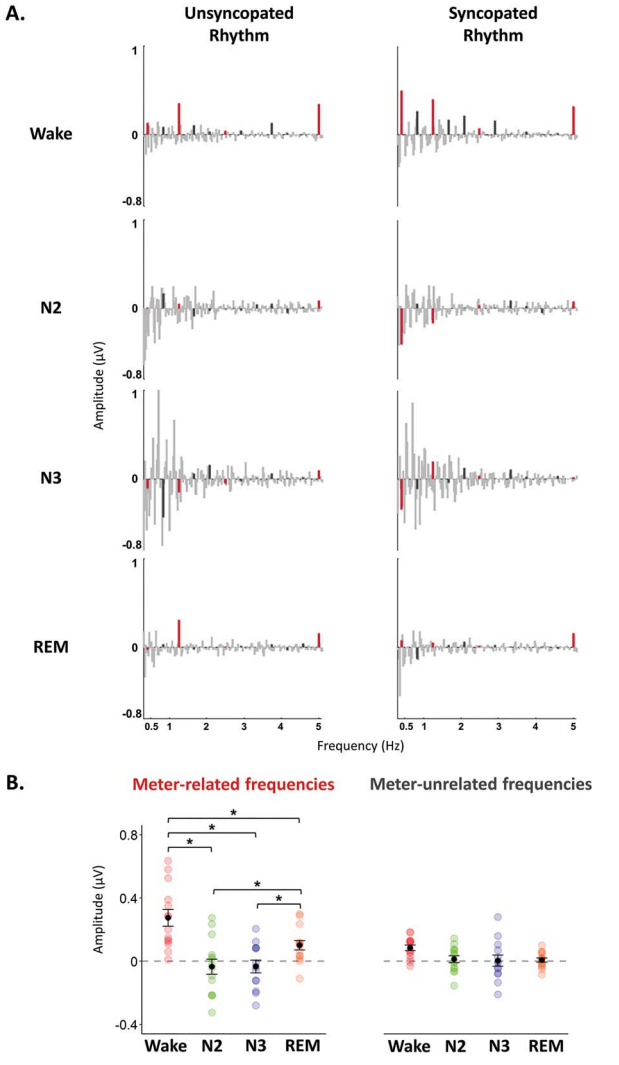

Figure 2. Cortical responses to the rhythms during wakefulness and sleep. Noise-subtracted spectral amplitudes in response to the unsyncopated and syncopated rhythms across states. (*A*) Averaged EEG spectra across all channels and participants (Wake, N2, and REM: $n = 14$; N3: $n = 13$) with responses at meter-related (red), and meter-unrelated (black) frequencies contained in the envelope of the rhythmic patterns. These responses were more prominent during wakefulness as compared to NREM and REM sleep. (*B*) Significant interaction between sleep stages and relative prominence of meter-related frequencies showing that, irrespective of rhythm complexity, responses at meter-related frequencies are significantly attenuated from wake to all sleep stages. These responses were suppressed during NREM sleep N2 and N3 and partially re-emerged during REM sleep. Asterisks denote significant differences ($P < 0.01$) after FDR correction.

Responses to the rhythms during NREM sleep stages N2 and N3 remained nonsignificant for meter-related frequencies ($Ps > 0.19$, BFs_{01} range 0.83–5.36; Supplementary Table 1).

To test the possibility that EEG responses to the rhythms may be significantly driven by involuntary head movements while participants listened to the rhythms in the wake condition, we analyzed the bipolar derivations of the EMG and EOG signals following the same procedure as the one used for EEG frequency-tagged responses as described above. Amplitude values at the frequencies of interest in both rhythms were nonsignificant in both the EMG and EOG channels (all $Ps > 0.29$, BFs_{01} range 0.82–5.97; Supplementary Table 2).

Table 3 Cortical responses elicited by syncopated and unsyncopated rhythmic sequences

	Unsyncopated rhythm	T	P	BF_{01}	Syncopated rhythm	t	P	BF_{01}
Meter-related frequencies								
Wake	0.211 ± 0.059	3.58	**0.008**	0.04	0.337 ± 0.076	4.44	**0.005**	0.01
Stage 2	0.049 ± 0.088	0.55	0.53	2.35	−0.118 ± 0.058	−2.04	0.97	9.35
Stage 3	−0.048 ± 0.065	−0.74	0.81	5.66	−0.018 ± 0.077	−0.24	0.73	4.24
REM	0.126 ± 0.060	2.10	0.08	0.36	0.076 ± 0.035	2.17	0.08	0.33
Meter-unrelated frequencies								
Wake	0.056 ± 0.014	4.16	**0.01**	0.01	0.113 ± 0.031	3.63	**0.008**	0.03
Stage 2	0.011 ± 0.037	0.29	0.57	2.95	0.014 ± 0.027	0.53	0.53	2.39
Stage 3	−0.015 ± 0.037	−0.40	0.74	4.69	0.022 ± 0.052	0.41	0.54	2.58
REM	0.014 ± 0.017	0.82	0.48	1.8	0.002 ± 0.015	0.14	0.60	3.33

Mean ± SEM of amplitude values (in μV) after noise subtraction. One-sample *t*-tests against zero (one-tailed) disclosed significant frequency-tagged cortical responses elicited at frequencies (both meter-related and -unrelated) of the envelope modulation spectra of the unsyncopated and syncopated rhythms during wakefulness. Responses at meter-related frequencies for both rhythms seemed to be elicited during REM sleep ($BF_{01} < 0.33$), but *P*-values were no longer significant after FDR correction. In contrast, noise-subtracted amplitude values in NREM sleep stages 2 and 3 were not significantly different from zero. Bayes factors (BF_{01}) provide a further characterization of null findings ($BF_{01} > 3$). Statistically significant *P*-values after FDR correction are shown in bold.

To additionally investigate brainstem-related (i.e., frequency-following responses) responses, we first focused on the overall response magnitude elicited at partial frequencies (f1, f2, f3), distortion products (f2 − f1, f3 − f1, and f3 − f2), and their surrounding sidebands during wakefulness. No significant frequency-following responses to the partials ($Ps > 0.78$, $BFs_{01} > 5.97$) nor to the distortion products ($Ps > 0.26$, all $BFs_{01} > 2.1$) were elicited by the presentation of the rhythms during wakefulness. In contrast, significant responses at sidebands surrounding the partials and distortion products were found in the wake condition for the unsyncopated rhythm ($t_{13} = 2.86$, $P = 0.007$), while responses at sideband frequencies for the syncopated rhythm during wake did not reach significance ($t_{13} = 1.6$, $P = 0.07$, $BF_{01} = 0.7$). Overall, the inconsistent pattern of results for frequency-following responses to rhythms during wake hindered the possibility to further compare the relative change between low- and high-level (i.e., envelope following responses) representations of the rhythms across wake and sleep states. The relatively low sound intensity chosen here for stimulus presentation in order not to awaken participants (i.e., ~45 dB) may have led to decreased amplitudes of the brainstem responses (Skoe and Kraus 2010) and may thus account for the poor signal-to-noise ratio in frequency-following responses to the rhythms, as opposed to previous studies (Nozaradan et al. 2018; Lenc et al. 2020). Therefore, subsequent analyses are only focused on cortical (envelope-following) responses across conditions.

Responses at Meter-Related Frequencies versus Meter-Unrelated Frequencies of the Rhythms in Wakefulness and Sleep

After assessing the responses to envelope frequencies elicited by the rhythms during wakefulness and sleep, we further investigated the relative enhancement of noise-subtracted amplitudes at meter-related versus meter-unrelated frequencies across rhythms and states.

A linear mixed model including state (wake, N2, N3, REM), meter (meter-related, meter-unrelated frequencies), rhythm complexity (unsyncopated, syncopated) and interactions as fixed effects, and random intercepts for each participant (model expressed as: amplitude ~ rhythm * state * meter + (1|Participant)) revealed a significant main effect of state ($F_{3,14726} = 13.11$, $P < 0.0001$), nonsignificant main effects of meter ($P = 0.09$), or rhythm complexity ($P = 0.84$) and a significant interaction between state and meter ($F_{3,14714} = 5.503$, $P < 0.001$). None of the interactions involving the factor rhythm complexity were significant ($Ps > 0.17$), including the triple interaction ($P = 0.49$).

Post hoc tests of amplitude values collapsed across rhythms and corrected for multiple comparisons with FDR showed that EEG frequency-tagged responses to the meter-related frequencies were enhanced during wakefulness as compared to NREM sleep N2 ($\beta = 0.31$, $t = 6.29$, $P < 0.001$) and N3 ($\beta = 0.3$, $t = 6.25$, $P < 0.001$), and REM sleep ($\beta = 0.16$, $t = 3.36$, $P = 0.003$). Moreover, responses at meter frequencies during REM sleep were significantly larger as compared to N2 ($\beta = 0.14$, $t = 2.96$, $P = 0.007$) and N3 ($\beta = 0.14$, $t = 2.95$, $P = 0.007$) of NREM sleep (Fig. 2B), and these responses were not significantly different between N2 and N3 stages ($P = 0.95$). In contrast, responses at meter-unrelated frequencies did not significantly differ across states ($Ps > 0.22$). Furthermore, responses at meter-related frequencies were selectively enhanced over meter-unrelated frequencies during wakefulness ($\beta = 0.18$, $t = 3.66$, $P = 0.001$), which was no longer the case during all sleep states ($Ps > 0.11$).

Finally, we conducted an exploratory analysis on the response amplitudes measured at the 4 individual meter-related frequencies (i.e., 0.4166, 1.25, 2.5, and 5 Hz) separately for each rhythm during wakefulness and REM sleep (Table 4). This analysis highlighted the presence of responses to the unsyncopated rhythm during both wakefulness and REM sleep, which remained significant after FDR correction, whereas responses to the syncopated rhythm were present during wakefulness but were no longer significant during REM sleep, except for the 5 Hz frequency ($P = 0.001$) corresponding to the 200 ms event rate within the auditory sequence.

Overall, our results indicate that, for both rhythms, meter-related responses that are present during wakefulness are selectively attenuated in REM sleep and further suppressed in NREM sleep. While the main analysis did not disclose differences across the unsyncopated and syncopated rhythms across states, an exploratory analysis of responses at individual meter frequencies of the rhythms suggests that the decrease of responses to the meter may be larger for the syncopated rhythm in which meter perception is not supported by prominent acoustic cues.

Table 4 Cortical responses at meter-related frequencies during wake and REM sleep

	Unsyncopated rhythm	t	P	BF_{01}	Syncopated rhythm	t	P	BF_{01}
Wakefulness								
0.416 Hz	0.134 ± 0.155	0.86	0.2	1.72	0.495 ± 0.218	2.27	**0.02**	0.28
1.25 Hz	0.352 ± 0.102	3.46	**0.002**	0.04	0.398 ± 0.117	3.41	**0.002**	0.05
2.5 Hz	0.047 ± 0.056	0.83	0.21	1.78	0.072 ± 0.050	1.44	0.09	0.88
5 Hz	0.348 ± 0.052	6.67	**0.001**	0.0003	0.317 ± 0.060	5.26	**0.001**	0.003
REM sleep								
0.416 Hz	−0.021 ± 0.165	–0.13	0.55	4.05	0.082 ± 0.122	0.67	0.26	2.08
1.25 Hz	0.311 ± 0.068	4.56	**0.001**	0.008	0.058 ± 0.055	1.04	0.16	1.41
2.5 Hz	0.010 ± 0.061	0.17	0.43	3.26	0.019 ± 0.035	0.53	0.30	2.39
5 Hz	0.163 ± 0.045	3.60	**0.002**	0.04	0.160 ± 0.036	4.45	**0.001**	0.009

Mean ± SEM of amplitude values (in μV) after noise subtraction. One-sample *t*-tests against zero (one-tailed) on responses corresponding to each meter-related frequency of the unsyncopated and syncopated rhythms. Note that significant responses to the unsyncopated rhythm were elicited during wakefulness and REM sleep, whereas responses to the syncopated rhythm were present during wakefulness but to a lesser extent during REM sleep. Bayes factors (BF_{01}) are provided to further characterize null findings. Statistically significant *P*-values after FDR correction are shown in bold.

Discussion

Here, we investigated whether higher-order representations of musical meter reflected by the relative prominence of EEG frequency-tagged responses at meter-related frequencies versus meter-unrelated frequencies emerge while exposed to repeated auditory rhythms during distinct stages of sleep and wakefulness. Our results show significant frequency-tagged responses to the meter of auditory rhythms during wakefulness and to a lesser extent during REM sleep. In contrast, such responses were abolished in stages 2 and 3 of NREM sleep. Moreover, a selective enhancement of neural responses at meter frequencies over meter-unrelated frequencies was observed for both rhythms during wakefulness, even for the syncopated rhythm where the meter frequencies are not prominent in the acoustic input, but this was no longer evident during NREM and REM sleep. These data thus show a reduced capacity to enhance metrical features in response to musical rhythms during REM sleep regardless of the prominence of these metrical features in the rhythmic stimulus.

Frequency-Tagged Responses to Rhythm Are Elicited during Wakefulness

Our results align with prior findings (Nozaradan et al. 2012, 2017, 2018; Lenc et al. 2018) showing that neural activity can synchronize to the acoustic envelope of rhythmic sequences during wakefulness, as reflected by significant EEG frequency-tagged responses at the corresponding frequencies contained in the envelope spectrum of each rhythm. Moreover, we found a relative enhancement of responses at meter-related frequencies when compared to responses elicited at meter-unrelated frequencies for both rhythms during wakefulness, again in line with prior studies (Nozaradan et al. 2012, 2017, 2018; Lenc et al. 2018). Responses at meter-related frequencies were enhanced even in response to the syncopated rhythm where the acoustic energy at the meter frequencies was not prominent in the modulation spectrum of the input, supporting the notion that meter perception relies on an neural representation that may not necessarily be driven by prominent acoustic features of the sound sequence (Chapin et al. 2010; Large et al. 2015; Tal et al. 2017; Lenc et al. 2020). The selective enhancement of neural responses at meter frequencies, even when these frequencies are not prominent in the acoustic sequence, suggests the existence of intrinsic mechanisms involved in high-level temporal representation of musical sequences that cannot be fully explained by the physical properties of the stimulus or physiological properties of subcortical auditory neurons (Large et al. 2015; Tal et al. 2017).

Frequency-Tagged Responses to Rhythm during Sleep

The investigation of these neural responses to rhythm was further extended here to NREM and REM sleep states. We found that different sleep stages lead to selective attenuation of the response, especially at meter-related frequencies. First, the presentation of the unsyncopated and syncopated rhythms did not elicit significant EEG frequency-tagged responses during NREM sleep stages 2 and 3. Previous studies using steady-state evoked potentials (SSEPs), in which periodic changes in voltage amplitude of the EEG signal are driven by repetitive fixed-rate stimulation (Regan 1966), showed that SSEPs progressively decrease as NREM sleep deepens (Picton et al. 2003) and are overall reduced as compared to both wakefulness (Cohen et al. 1991; Picton et al. 2003; Tlumak et al. 2012; Lustenberger et al. 2018; Sharon and Nir 2018; Górska and Binder 2019) and REM sleep (Cohen et al. 1991). Auditory SSEPs during NREM sleep have been investigated using a wide range of amplitude-modulated tone burst rates, and studies consistently found a reduction in responses during NREM sleep for high (32–80 Hz; Cohen et al. 1991; Picton et al. 2003; Tlumak et al. 2012; Lustenberger et al. 2018; Górska and Binder 2019) and low stimulation rates ranging 4–20 Hz (Lustenberger et al. 2018; Górska and Binder 2019; but see Tlumak et al. 2012). Furthermore, the presentation of periodic stimulation during NREM sleep, particularly within the range of slow oscillations (SOs; 0.5–4 Hz) and sleep spindles (11–16 Hz), induces an increase of these oscillatory phenomena specific to sleep (Ngo et al. 2013; Antony and Paller 2017; Lustenberger et al. 2018; Simor, Steinbach, et al. 2018b). For instance, presentation of amplitude-modulated sounds in a frequency range corresponding to sleep spindles was found to increase the amount of spindles and spindle activity during and shortly after the stimulation period (Antony and Paller 2017; Lustenberger et al. 2018), as well as SO density in comparison with subsequent stimulation periods (Antony and Paller 2017). Also, frequency-specific SSEPs are reduced during periods of stimulation containing spindles (Lustenberger et al. 2018), suggesting that fixed-rate stimulation at spindle frequencies prompts a global response in the

thalamocortical system (i.e., increase in sleep spindle and slow wave activity), rather than a steady-state response restricted to a specific frequency.

It has been proposed that sleep spindles play an important role in gating the transmission of incoming sensory information, thus preventing the organism from awakening (Steriade et al. 1993). Evidence from EEG and neuroimaging studies shows that the oscillatory hallmarks of NREM sleep such as sleep spindles and SOs modulate brain responses to auditory stimuli. For instance, sound presentation concurrent with sleep spindles elicits a higher late ERP positivity (Elton et al. 1997; Cote et al. 2000) that further increases with sound intensity (Cote et al. 2000), an effect thought to reflect inhibition of information processing. Moreover, fMRI studies showed that wake-like responses to tones persist in the thalamus and auditory primary cortex during NREM sleep when sounds are delivered without concurrent spindles (Dang-Vu et al. 2011; Schabus et al. 2012). Notwithstanding, the notion that spindles play a role in inhibiting incoming sensory information during sleep has been challenged by intracortical EEG studies in rodents and humans suggesting a lack of modulation by spindles detected at thalamic and cortical levels on cortical responses to auditory (Sela et al. 2016) and nociceptive (Claude et al. 2015) stimulation as compared to stimulation periods without spindles. Furthermore, modulation of firing rates of cortical neurons during sleep spindles was not consistent in intracranial human recordings (Andrillon et al. 2011), as opposed to the modulation of cortical firing rates observed during the upstate of slow waves (Nir et al. 2011). Sleep spindles may not be the only neurophysiological feature of NREM sleep underlying sensory disconnection from the environment. During deep sleep, sensory information may not be effectively driven from primary to higher-order regions due to functional cortical disconnection (Massimini et al. 2005) and transient windows of excitability during the upstates of the SO, which modulate the propagation of incoming information (Bergmann et al. 2012; Schabus et al. 2012). For instance, stimulus presentation toward the upstate of a SO elicited increased activation in auditory association cortices (Schabus et al. 2012) and led to greater ERP late-positivity and delayed increases in spindle and beta power, as compared to tones delivered toward the downstate (Schabus et al. 2012; Cox et al. 2014). The pervasiveness of sleep spindles and SOs, both spontaneous and induced (e.g., K-complexes), during NREM sleep stages 2 and 3 may explain why we did not observe neural responses synchronizing with the envelope frequencies of both rhythms. The relatively long duration of our stimulation trials and the fact that we did not deliver a higher number of repetitions throughout the night may have prevented us from averaging out widespread evoked K-complex activity and other NREM-specific features. In contrast with studies demonstrating a residual capacity of the brain to respond to periodic fixed-rate stimulation, or to discriminate salient or novel information during NREM sleep, the lack of frequency-tagged responses to the envelope of the rhythmic sequences used in this study may also be explained by the fact that the stimuli were not strictly isochronous but consisted in relatively complex rhythmic sequences that require the extraction of a high-order temporal structure over time. Overall, these findings are in line with the notion that responsiveness to auditory stimuli during NREM sleep is constrained by momentary oscillatory features preventing complex auditory sequences from being processed in their entirety, further hindering processing at higher-order levels.

An alternative explanation for the lack of EEG responses to rhythms observed in the current study could be that these frequency-tagged responses were partially masked by the prominent oscillatory activity typically observed in NREM sleep within the range of SOs. However, responses to the envelope of the rhythms during NREM sleep stages 2 and 3 remained clearly nonsignificant after discarding the slowest meter-related frequency (0.416 Hz) from the analyses, suggesting that slow activity, at least within the slowest range of oscillatory activity of NREM sleep (<1 Hz), does not fully explain the differences in EEG responses to non-isochronous rhythms observed across sleep stages.

Contrary to NREM sleep observations, during REM sleep responses to meter-related frequencies were larger than in NREM sleep for both rhythms, although these responses were weaker than during wakefulness. REM sleep is a state characterized by low-voltage mixed-frequency EEG patterns of activity, where neocortical neurons are tonically depolarized, as is the case during wakefulness (Steriade et al. 2001). Studies on auditory processing during REM sleep reported differential brain responses to salient or relevant stimuli (Atienza et al. 2001; Bastuji et al. 2002), suggesting that the REM sleeping brain is not entirely disconnected from its environment and continues evaluating external information to some extent (Blume et al. 2018). Our finding that neural responses to relatively long periods of auditory presentation of musical rhythms can be elicited during REM sleep is in line with previous studies showing the preserved processing of long streams of informative versus meaningless speech (Koroma et al. 2020), and parsing of syllables within sentences (Makov et al. 2017). It should be kept in mind, however, that REM sleep is further divided into tonic and phasic periods of activity, the latter being characterized by bursts of REMs (Simor et al. 2020). In contrast with phasic REM, tonic periods of REM sleep are characterized by lower arousal thresholds (Ermis et al. 2010), enhanced responsiveness to auditory stimulation (Sallinen et al. 1996; Takahara et al. 2002; Koroma et al. 2020), and residual activation of the auditory cortex during sound presentation (Wehrle et al. 2007). Moreover, sustained auditory stimulation significantly decreases the occurrence of REMs in REM sleep (Wehrle et al. 2007; Stuart and Conduit 2009), supporting the notion of an increased environmental alertness during tonic REM sleep (Simor, Gombos, et al. 2018a). Although rhythmic sequences were not presented during separate tonic and phasic periods of REM sleep, these prior studies suggest that enhanced responses to the meter of both rhythms are most likely elicited during tonic REM sleep. In a recent study, evoked responses to deviant tones were elicited during both tonic and phasic periods of REM sleep during a first but not a second night in the laboratory where differential processing of deviants only persisted in tonic REM sleep (Tamaki and Sasaki 2019). Accordingly, our results may reflect an increased engagement of the sleeper toward the novel environment during REM sleep. Future studies should clarify the role of tonic and phasic REM sleep in the processing of complex acoustic stimuli during and after an adaptation night in a new environment such as the sleep laboratory.

Selective Attenuation of Meter Frequencies across Sleep Stages, Irrespective of Overall Attenuation of Responsiveness to Sound

Our results suggested selective attenuation of the responses at meter-related frequencies across different sleep stages.

However, this is not simply due to overall decrease of the responsiveness to sound, as attenuation was not observed for meter-unrelated frequencies. Most importantly, this attenuation occurred even in the irregular rhythm in which the meter-related frequencies were not prominent in the stimulus, thus suggesting that the neural processes selectively enhancing meter-related frequencies during wakefulness were weakened during REM and further suppressed in NREM stages.

These results are in line with previous work showing that while the ability to track basic features in complex and continuous auditory streams may be to some extent preserved during sleep, integrating higher-level representations of such inputs is hampered during NREM sleep. For example, a study using an auditory local–global paradigm showed preserved bottom-up sensory adaptation to local changes in auditory streams, whereas top-down detection of violations to global regularities was abolished as early as stage 1 of NREM sleep (Strauss et al. 2015). Using the frequency-tagging approach to investigate high-order detection of statistical regularities embedded in auditory streams during NREM sleep, Farthouat et al. (2018) showed that like in wakefulness, responses tagged to the tone presentation rate (at 5.505 Hz) persist during NREM sleep but found no evidence of the segmentation of the statistical streams (grouping of tri-tones at 1.835 Hz) even though participants exhibited this capacity when awake. Similarly, the capacity to parse continuous speech streams according to distinct hierarchical levels is disrupted during sleep (Makov et al. 2017). Namely, by presenting speech sequences containing syllables, words, phrases, and sentences presented at fixed rates (i.e., hierarchical linguistic levels corresponded to distinct frequencies), Makov et al. (2017) found neural responses at the syllabic rate of intelligible and unintelligible speech streams during NREM and REM sleep, while neural responses to higher-order linguistic levels were abolished during sleep. Accordingly, it has been shown that although presentation of linguistic material during NREM sleep elicits activation at thalamic and primary auditory cortical levels, brain activation progressively diminishes along the hierarchy of language processing (Portas et al. 2000; Wilf et al. 2016). Moreover, in this study, we did not find significant differences in high-order responses to meter frequencies between stages 2 and 3 of NREM sleep, as opposed to previous studies showing that electrophysiological responses associated with high-order processes such as correct semantic categorization of a previously automatized task (Kouider et al. 2014; Andrillon et al. 2016) or selective amplification of meaningful over noninformative competing speech streams (Legendre et al. 2019) can be found during light stage 2, NREM, whereas these responses vanish in deeper stage 3 of NREM sleep. These discrepancies may be explained by contextual and task-related differences across stimuli and experiments (Andrillon and Kouider 2020) and speak of the dynamic nature of auditory processing across vigilance stages (Arzi et al. 2021; Wielek et al. 2021).

While the present study adds to our understanding of the perceptual capabilities of the sleeping brain, several limitations need to be acknowledged. First, the limited sample size in our study ($N = 14$) may explain the lack of significant differences between rhythms in the linear mixed model. Increased power in subsequent studies with larger sample size will be relevant to further confirm our findings and examine potential differences between responses to rhythms that vary in complexity while controlling for low-level acoustic confounds. Second, we recorded a small number of electrodes, limiting the possibility to investigate topographical differences in the frequency-tagged responses to rhythms across states. Studies with high-density EEG could provide additional information on the spatial distribution of responses to musical rhythm and how it changes depending on the underlying neurophysiological state.

Conclusions

In the present study, we evidence state-dependent changes in the neurophysiological activity subtending the emergence of high-order representations of temporal structures such as the meter of complex rhythmic sequences. EEG frequency-tagged responses to both simple unsyncopated and complex syncopated rhythms were observed during wakefulness, found partially preserved during REM sleep, and abolished during NREM sleep. The neural capacity to respond at metrical frequencies during REM sleep is reduced even for syncopated rhythms in which the internal representation of the meter cannot be simply explained by low-level sensory processing of acoustic features of the input. Consequently, our results support the proposal that the capacity to process auditory streams during sleep is limited by the underlying neurophysiological organization.

Supplementary Material

Supplementary material can be found at *Cerebral Cortex* online.

Funding

Fonds de la Recherche Scientifique (F.R.S.-F.N.R.S., Aspirant Research Fellowship to R.S.O.); F.N.R.S. and the Fonds Wetenschappelijk Onderzoek – Vlaanderen (F.W.O.) under the Excellence of Science (EOS) Project (MEMODYN, No. 30446199 to P.P.).

Notes

Conflict of Interest: None declared.

References

Andrillon T, Kouider S. 2020. The vigilant sleeper: neural mechanisms of sensory (de)coupling during sleep. *Curr Opin Physiol*. 15:47–59.

Andrillon T, Nir Y, Staba RJ, Ferrarelli F, Cirelli C, Tononi G, Fried I. 2011. Sleep spindles in humans: insights from intracranial EEG and unit recordings. *J Neurosci*. 31:17821–17834.

Andrillon T, Poulsen AT, Hansen LK, Léger D, Kouider S. 2016. Neural markers of responsiveness to the environment in human sleep. *J Neurosci*. 36:6583–6596.

Antony JW, Paller KA. 2017. Using oscillating sounds to manipulate sleep spindles. *Sleep*. 40:zsw068.

Arzi A, Trentin C, Laudini A, Krugliak A, Nikolla D, Bekinschtein T. 2021. Dynamic auditory remapping across the sleep-wake cycle. *bioRxiv*. 2021.02.16.431383:1–55.

Atienza M, Cantero JL, Escera C. 2001. Auditory information processing during human sleep as revealed by event-related brain potentials. *Clin Neurophysiol*. 112:2031–2045.

Bastuji H, Perrin F, Garcia-Larrea L. 2002. Semantic analysis of auditory input during sleep: studies with event related potentials. *Int J Psychophysiol*. 46:243–255.

Bates D, Mächler M, Bolker B, Walker S. 2015. Fitting linear mixed-effects models using lme4. *J Stat Softw*. 67:1–48.

Benjamini Y, Hochberg Y. 1995. Controlling the false discovery rate: a practical and powerful approach to multiple testing. *J R Stat Soc Ser B*. 57:289–300.

Bergmann TO, Mölle M, Schmidt MA, Lindner C, Marshall L, Born J, Siebner HR. 2012. EEG-guided transcranial magnetic stimulation reveals rapid shifts in motor cortical excitability during the human sleep slow oscillation. *J Neurosci*. 32:243–253.

Berry RB, Brooks R, Gamaldo CE, Harding SM, Lloyd RM, Quan SF, Troester MM, Vaughn BV. 2017. *The AASM manual for the scoring of sleep and associated events: rules, terminology and technical specifications. Version 2.4*. Darien (IL): American Academy of Sleep Medicine.

Blume C, del Giudice R, Wislowska M, Heib DPJ, Schabus M. 2018. Standing sentinel during human sleep: continued evaluation of environmental stimuli in the absence of consciousness. *NeuroImage*. 178:638–648.

Brainard DH. 1997. The Psychophysics Toolbox. *Spat Vis*. 10:433–436.

Buysse DJ, Reynolds CF, Monk TH, Berman SR, Kupfer DJ. 1989. The Pittsburgh Sleep Quality Index: a new instrument for psychiatric practice and research. *Psychiatry Res*. 28:193–213.

Chapin HL, Zanto T, Jantzen KJ, Kelso SJA, Steinberg F, Large EW. 2010. Neural responses to complex auditory rhythms: the role of attending. *Front Psychol*. 1:224.

Chatrian GE, Lettich E, Nelson PL. 1985. Ten percent electrode system for topographic studies of spontaneous and evoked EEG activities. *Am J EEG Technol*. 25:83–92.

Claude L, Chouchou F, Prados G, Castro M, De Blay B, Perchet C, García-Larrea L, Mazza S, Bastuji H. 2015. Sleep spindles and human cortical nociception: a surface and intracerebral electrophysiological study. *J Physiol*. 593:4995–5008.

Coffey EBJ, Nicol T, White-Schwoch T, Chandrasekaran B, Krizman J, Skoe E, Zatorre RJ, Kraus N. 2019. Evolving perspectives on the sources of the frequency-following response. *Nat Commun*. 10:1–10.

Cohen LT, Rickards FW, Clark GM. 1991. A comparison of steady-state evoked potentials to modulated tones in awake and sleeping humans. *J Acoust Soc Am*. 90:2467–2479.

Cote KA, Epps TM, Campbell KB. 2000. The role of the spindle in human information processing of high-intensity stimuli during sleep. *J Sleep Res*. 9:19–26.

Cox R, Korjoukov I, De Boer M, Talamini LM. 2014. Sound asleep: processing and retention of slow oscillation phase-targeted stimuli. *PLoS One*. 9:e101567.

Daltrozzo J, Claude L, Tillmann B, Bastuji H, Perrin F. 2012. Working memory is partially preserved during sleep. *PLoS One*. 7:e50997.

Dang-Vu TT, Bonjean M, Schabus M, Boly M, Darsaud A, Desseilles M, Degueldre C, Balteau E, Phillips C, Luxen A, et al. 2011. Interplay between spontaneous and induced brain activity during human non-rapid eye movement sleep. *Proc Natl Acad Sci U S A*. 108:15438–15443.

Dienes Z. 2014. Using Bayes to get the most out of non-significant results. *Front Psychol*. 5:781.

Elton M, Winter O, Heslenfeld D, Loewy D, Campbell K, Kok A. 1997. Event-related potentials to tones in the absence and presence of sleep spindles. *J Sleep Res*. 6:78–83.

Ermis U, Krakow K, Voss U. 2010. Arousal thresholds during human tonic and phasic REM sleep: phasic and tonic REM sleep. *J Sleep Res*. 19:400–406.

Farthouat J, Atas A, Wens V, De Tiege X, Peigneux P. 2018. Lack of frequency-tagged magnetic responses suggests statistical regularities remain undetected during NREM sleep. *Sci Rep*. 8:1–16.

Fox J, Weisberg S. 2019. *An R companion to applied regression*. 3rd ed. Thousand Oaks (CA): Sage.

Górska U, Binder M. 2019. Low and medium frequency auditory steady-state responses decrease during NREM sleep. *Int J Psychophysiol*. 135:44–54.

Horne JA, Östberg O. 1976. A self-assessment questionnaire to determine morningness-eveningness in human circadian rhythms. *Int J Chronobiol*. 4:97–110.

Issa EB, Wang X. 2008. Sensory responses during sleep in primate primary and secondary auditory cortex. *J Neurosci*. 28:14467–14480.

Koroma M, Lacaux C, Andrillon T, Legendre G, Léger D, Kouider S. 2020. Sleepers selectively suppress informative inputs during rapid eye movements. *Curr Biol*. 30:2411–2417.e3.

Kouider S, Andrillon T, Barbosa LS, Goupil L, Bekinschtein TA. 2014. Inducing task-relevant responses to speech in the sleeping brain. *Curr Biol*. 24:2208–2214.

Large EW, Herrera JA, Velasco MJ. 2015. Neural networks for beat perception in musical rhythm. *Front Syst Neurosci*. 9:159.

Legendre G, Andrillon T, Koroma M, Kouider S. 2019. Sleepers track informative speech in a multitalker environment. *Nat Hum Behav*. 3:274–283.

Lenc T, Keller PE, Varlet M, Nozaradan S. 2018. Neural tracking of the musical beat is enhanced by low-frequency sounds. *Proc Natl Acad Sci U S A*. 115:8221–8226.

Lenc T, Keller PE, Varlet M, Nozaradan S. 2020. Neural and behavioral evidence for frequency-selective context effects in rhythm processing in humans. *Cereb Cortex Commun*. 1:tgaa037.

Lenc T, Merchant H, Keller PE, Honing H, Varlet M, Nozaradan S. 2021. Mapping between sound, brain and behavior: four-level framework for understanding rhythm processing in humans and non-human primates. *Philos Trans R Soc B Biol Sci*. 376:20200325.

Lenth RV. 2021. emmeans: Estimated Marginal Means, aka Least-Squares Means. R package version 1.6.1. https://CRAN.R-project.org/package=emmeans (last accessed 22 July 2021).

Lustenberger C, Patel YA, Alagapan S, Page JM, Price B, Boyle MR, Fröhlich F. 2018. High-density EEG characterization of brain responses to auditory rhythmic stimuli during wakefulness and NREM sleep. *NeuroImage*. 169:57–68.

Makov S, Sharon O, Ding N, Ben-Shachar M, Nir Y, Golumbic EZ. 2017. Sleep disrupts high-level speech parsing despite significant basic auditory processing. *J Neurosci*. 37:7772–7781.

Massimini M, Ferrarelli F, Huber R, Esser SK, Singh H, Tononi G. 2005. Neuroscience: breakdown of cortical effective connectivity during sleep. *Science (80-)*. 309:2228–2232.

Meltzer B, Reichenbach CS, Braiman C, Schiff ND, Hudspeth AJ, Reichenbach T. 2015. The steady-state response of the cerebral cortex to the beat of music reflects both the comprehension of music and attention. *Front Hum Neurosci*. 9:436.

Mouraux A, Iannetti GD, Colon E, Nozaradan S, Legrain V, Plaghki L. 2011. Nociceptive steady-state evoked potentials elicited by rapid periodic thermal stimulation of cutaneous nociceptors. *J Neurosci*. 31:6079–6087.

Ngo HVV, Claussen JC, Born J, Mölle M. 2013. Induction of slow oscillations by rhythmic acoustic stimulation. *J Sleep Res*. 22:22–31.

Nir Y, Staba RJ, Andrillon T, Vyazovskiy VV, Cirelli C, Fried I, Tononi G. 2011. Regional slow waves and spindles in human sleep. *Neuron*. 70:153–169.

Nir Y, Vyazovskiy VV, Cirelli C, Banks MI, Tononi G. 2015. Auditory responses and stimulus-specific adaptation in rat auditory cortex are preserved across NREM and REM sleep. *Cereb Cortex*. 25:1362–1378.

Nozaradan S. 2014. Exploring how musical rhythm entrains brain activity with electroencephalogram frequency-tagging. *Philos Trans R Soc B Biol Sci*. 369:20130393.

Nozaradan S, Mouraux A, Jonas J, Colnat-Coulbois S, Rossion B, Maillard L. 2017. Intracerebral evidence of rhythm transform in the human auditory cortex. *Brain Struct Funct*. 222:2389–2404.

Nozaradan S, Peretz I, Missal M, Mouraux A. 2011. Tagging the neuronal entrainment to beat and meter. *J Neurosci*. 31:10234–10240.

Nozaradan S, Peretz I, Mouraux A. 2012. Selective neuronal entrainment to the beat and meter embedded in a musical rhythm. *J Neurosci*. 32:17572–17581.

Nozaradan S, Schönwiesner M, Caron-Desrochers L, Lehmann A. 2016. Enhanced brainstem and cortical encoding of sound during synchronized movement. *NeuroImage*. 142: 231–240.

Nozaradan S, Schönwiesner M, Keller PE, Lenc T, Lehmann A. 2018. Neural bases of rhythmic entrainment in humans: critical transformation between cortical and lower-level representations of auditory rhythm. *Eur J Neurosci*. 47:321–332.

Peña JL, Pérez-Perera L, Bouvier M, Velluti RA. 1999. Sleep and wakefulness modulation of the neuronal firing in the auditory cortex of the guinea pig. *Brain Res*. 816:463–470.

Perrin F, García-Larrea L, Mauguière F, Bastuji H. 1999. A differential brain response to the subject's own name persists during sleep. *Clin Neurophysiol*. 110:2153–2164.

Picton TW, John MS, Purcell DW, Plourde G. 2003. Human auditory steady-state responses: the effects of recording technique and state of arousal. *Anesth Analg*. 97:1396–1402.

Portas CM, Krakow K, Allen P, Josephs O, Armony JL, Frith CD. 2000. Auditory processing across the sleep-wake cycle: simultaneous EEG and fMRI monitoring in humans. *Neuron*. 28:991–999.

R Core Team (2019). R: A language and environment for statistical computing. R Foundation for Statistical Computing, Vienna, Austria. https://www.R-project.org/.

Regan D. 1966. Some characteristics of average steady-state and transient responses evoked by modulated light. *Electroencephalogr Clin Neurophysiol*. 20:238–248.

Sallinen M, Kaartinen J, Lyytinen H. 1996. Processing of auditory stimuli during tonic and phasic periods of REM sleep as revealed by event-related brain potentials. *J Sleep Res*. 5:220–228.

Schabus MD, Dang-Vu TT, Heib DPJ, Boly M, Desseilles M, Vandewalle G, Schmidt C, Albouy G, Darsaud A, Gais S. 2012. The fate of incoming stimuli during NREM sleep is determined by spindles and the phase of the slow oscillation. *Front Neurol*. 3:40.

Sela Y, Vyazovskiy VV, Cirelli C, Tononi G, Nir Y. 2016. Responses in rat core auditory cortex are preserved during sleep spindle oscillations. *Sleep*. 39:1069–1082.

Sharon O, Nir Y. 2018. Attenuated fast steady-state visual evoked potentials during human sleep. *Cereb Cortex*. 28:1297–1311.

Simor P, Gombos F, Blaskovich B, Bódizs R. 2018a. Long-range alpha and beta and short-range gamma EEG synchronization distinguishes phasic and tonic REM periods. *Sleep*. 41:zsx210.

Simor P, Steinbach E, Nagy T, Gilson M, Farthouat J, Schmitz R, Gombos F, Ujma PP, Pamula M, Bódizs R, et al. 2018b. Lateralized rhythmic acoustic stimulation during daytime NREM sleep enhances slow waves. *Sleep*. 41:zsy176.

Simor P, van der Wijk G, Nobili L, Peigneux P. 2020. The microstructure of REM sleep: why phasic and tonic? *Sleep Med Rev*. 52:101305.

Skoe E, Kraus N. 2010. Auditory brainstem response to complex sounds: a tutorial. *Ear Hear*. 31:302–324.

Steriade M, McCormick DA, Sejnowski TJ. 1993. Thalamocortical oscillations in the sleeping and aroused brain. *Science (80-)*. 262:679–685.

Steriade M, Timofeev I, Grenier F. 2001. Natural waking and sleep states: a view from inside neocortical neurons. *J Neurophysiol*. 85:1969–1985.

Strauss M, Sitt JD, King J-R, Elbaz M, Azizi L, Buiatti M, Naccache L, van Wassenhove V, Dehaene S. 2015. Disruption of hierarchical predictive coding during sleep. *Proc Natl Acad Sci*. 112:E1353–E1362.

Stuart K, Conduit R. 2009. Auditory inhibition of rapid eye movements and dream recall from REM sleep. *Sleep*. 32: 399–408.

Takahara M, Nittono H, Hori T. 2002. Comparison of the event-related potentials between tonic and phasic periods of rapid eye movement sleep. *Psychiatry Clin Neurosci*. 56: 257–258.

Tal I, Large EW, Rabinovitch E, Wei Y, Schroeder CE, Poeppel D, Golumbic EZ. 2017. Neural entrainment to the beat: The "missing-pulse" phenomenon. *J Neurosci*. 37: 6331–6341.

Tamaki M, Sasaki Y. 2019. Surveillance during REM sleep for the first-night effect. *Front Neurosci*. 13:1161.

Tierney A, Kraus N. 2014. Neural entrainment to the rhythmic structure of music. *J Cogn Neurosci*. 27:400–408.

Tlumak AI, Durrant JD, Delgado RE, Robert BJ. 2012. Steady-state analysis of auditory evoked potentials over a wide range of stimulus repetition rates in awake vs. natural sleep. *Int J Audiol*. 51:418–423.

Tranchant P, Vuvan DT, Peretz I. 2016. Keeping the beat: a large sample study of bouncing and clapping to music. *PLoS One*. 11:e0160178.

Wehrle R, Kaufmann C, Wetter TC, Holsboer F, Auer DP, Pollmächer T, Czisch M. 2007. Functional microstates within human REM sleep: first evidence from fMRI of a thalamocortical network specific for phasic REM periods. *Eur J Neurosci*. 25:863–871.

Wielek T, Blume C, Wislowska M, Del Giudice R, Schabus M. 2021. Decoding brain responses to names and voices across different vigilance states. *Sensors*. 21: 3393.

Wilf M, Ramot M, Furman-Haran E, Arzi A, Levkovitz Y, Malach R. 2016. Diminished auditory responses during NREM sleep correlate with the hierarchy of language processing. *PLoS One*. 11:e0157143.